Office of Naval Research

Contract N00014-89-J-1276

Technical Report No. UWA/DME/TR92/68

TEAR STRAPS IN AIRPLANE FUSELAGE

by

M. Kosai, A.S. Kobayashi and M. Ramulu

March 1992

The research reported in this technical report was made possible through support extended to the Department of Mechanical Engineering, University of Washington, by the Office of naval Research under Contract N00014-89-J-1276. Reproduction in whole or in part is permitted for any purpose of the United States Government.

Department of Mechanical Engineering

College of Engineering

University of Washington

MISSING PAGES WILL BE INSERTED AT AN LATER DATE
AS ERRATA(S)

TEAR STRAPS IN AIRPLANE FUSELAGE

M. Kosai, A. S. Kobayashi and M. Hamulu
University of Washington
Department of Mechanical Engineering
Seattle, Washington 98195

Abstract

A procedure based on dynamic fracture mechanics is proposed for assessing the effectiveness of tear straps in a rupturing airplane fuselage weakened by a row of multiple site damage (MSD). A large deformation, elastic-plastic finite element model of the rupturing fuselage with an unsymmetrical crack flap is used to demonstrate the existence of a mixed mode I and II crack tip deformation and a large axial stress preceding the propagating crack. These numerical results were used to evaluate the dynamic crack curving and crack arrest criteria and hence to assess the possibility of crack curving as the crack approaches a tear strap without the presence of MSD.

Introduction

The role of a tear strap in an airplane fuselage is to arrest an axial crack which is propagating either subcritically under fatigue loading or dynamically after reaching criticality. Such crack arrest can occur by the lower stresses due to the reinforcing effect of the tear strap or by crack curving due to the complex crack tip stress field generated by the crack flap and the tear strap. The latter provides controlled damage and depressurization of the fuselage Although the tear strap is the last defense of an axially rupturing fuselage, little is known about its effectiveness in arresting an axial crack and much of its design is based on empirical rules derived from sub- and full-scale testings of pressurized fuselages. Literature is abundant with analytical and experimental papers dealing with axial fatigue crack extension and possible arrest in idealized and actual fuselages but few consider crack curving and flapping as an arrest criterion. The only analytical paper dealing with tear straps and crack curving and flapping as an arrest criterion appears to be that of Kosai and Kobayashi (1991).

In the above mentioned paper, the axial crack was assumed to open symmetrically, i.e. mode I crack tip deformation, in a fuselage reinforced by longitudinal stringers, frames and tear straps. If failure were to occur along the multiple site damages (MSD's) in a lap joint, evidences [Sampath and Broek (1991); NTSB (1989)] show that fracture will occur only in the upper skin with the lower skin still attached to the fasteners. The axial stretching due to the resultant one-sided crack flap would then generate axial tensile stresses along the cracked upper skin and impose a mode II state of crack tip deformation.

The importance of mode II deformation and the attendant mode II stress intensity factor, K_{II}, was also observed recently in a fatigue crack growth study of a miniaturized and idealized model of a stringer reinforced fuselage by Fyfe and Sethi (1991).

The purpose of this study is to refine the finite element modelling of axial crack propagation and curving in a pressurized fuselage [Kosai and Kobayashi (1991)] by accounting for this more realistic mode II crack tip deformation.

Finite Element Modelling

Due to the unsymmetric crack tip deformation of an axial crack along a lap joint, one half of the airplane fuselage, as shown in Figure 1, must be modelled by finite elements. Implicit in this modelling is an assumption, which was made to reduce the computing time, that an identical axial crack was also propagating in the other symmetric half of the fuselage. The geometric parameters associated with the fuselage and the material properties of the 2024-T3 clad aluminum used in the skin and the tear strap are shown in Table 1.

One of the unknown quantity is the actual pressure distribution on as well as in the vicinity of the crack flap as it propagates. As shown in Figure 2, in one analysis, the crack flap was assumed to be loaded with the cabin pressure through the layer of cabin insulation which acted as a weak bladder and which maintains the cabin pressure during the short subsecond duration of rapid axial crack propagation. In another analysis, the effect of a leakage in cabin air was studied by prescribing a linearly decreasing pressure on the crack flap while maintaining the cabin pressure on the uncracked portion of the fuselage.

Figure 3 shows the finite element model (FEM) of the rupturing fuselage. The longitudinal stringers were modelled by beam elements, the frames were replaced with beam elements and the straps were represented by increased skin thickness. The limit cabin pressure differential of 51.7 kPa (7.5 psi) was prescribed. A quasi-static, elastic-plastic finite element analysis was used to model the rapid crack propagation in this ductile material. This quai-static analysis was justified since the measured crack velocities in the thicker and more brittle 7075-T6 and 7178-T6 aluminum plates was less than ten percent of the dilatational wave velocity [Kobayashi and Engstrom (1967); Arakawa, Drinnon, Kosai and Kobayashi (1991)].

Also the limit hoop stress in the uncracked skin of the fuselage is a low 1.06 MPa (15.4 ksi) and thus the computed crack tip plastic zone size is less than one of the coarse mesh element when the crack length less than a = 178 mm (7 in.). Thus, the prior history of plastic yielding for a crack length less than 178 mm (7 in.) was ignored and an incremental static, elastic-plastic finite element analysis was initiated at a = 178 mm

(7 in.) by advancing the crack tip one nodal distance, i.e. 25.4 mm (1 in.), and by superposing the prior elastic-plastic state to that after each crack advance.

The crack curving criterion, which is triggered as the crack approaches the tear strap is based on the near crack tip state of stress and thus considerable refinement of the finite element mesh was necessary to meet the required numerical accuracy. Refined mesh, on the other hand, increased exponentially the computation time of this incremental elastic-plastic analysis. In order to reduce the computer time, the crack tip region, where crack kinking was likely to occur, was first identified through a coarse mesh finite element analysis. This region was then reanalyzed with a refined mesh using a rezoning procedure as shown in Figure 3. This simulation of crack propagation was continued by incrementally advancing the crack tip using the coarse mesh model and by repeating the analysis with the refined mesh using the restart file generated from the coarse mesh model. The crack kinking angle was then computed and the kinked crack path was generated incrementally by using the refined mesh in the crack tip region using the restart file generated from previous analysis.

Crack Curving

As mentioned previously, the function of a tear strap is not so much as to arrest a propagating axial crack by reducing the circumferential stress in the crack path, but to deflect the crack in the circumferential direction. The large opening due to crack flapping would then reduce the crack driving force through controlled depressurization of the cabin and thus arrest the crack. Such crack deflection is accomplished by the presence of mode II stress intensity factor, K_{II}, which is generated by the flap of the upper skin. The large crack flap also generates a large axial stress ahead of the propagating crack tip [Kobayashi, Emery, Love and Chao (1988); Kobayashi, Emery, Love and Chao (1988)], and together with the reduced circumferential stress due to the presence of the tear strap augments the propensity for crack curving under mixed mode crack tip loading.

In a previous analysis [Kosai and Kobayashi (1991)], an elastic crack kinking criterion for a stationary mode I crack [9,10] with plasticity correction was used to assess the effectiveness of the tear strap for a symmetric crack flap. The unsymmetric crack flap considered in this study, however, will generate a combined mode I and II crack tip deformation field [Fyfe and Sethi (1991)] and thus crack kinking is inherent in such crack tip deformation.

If the apparent mode I stress intensity factor, K_I, is elevated by the presence of a row of MSD's along the axis of the crack, then the crack will continue to propagate in the axial direction despite the presence of an inevitable crack tip bulging and the resultant K_{II} in a pressurized fuselage [NTSB (1989)]. The physical evidence of such self similar crack extension along a row of MSD's in the presence of K_{II} thus requires a new crack curving criterion.

Using the maximum stress criterion with the crack tip stress field, the angle of crack kinking, θ_C in the presence of K_{II} was derived by Erdogan and Sih (1963). This maximizing condition yields

$$K_I \sin\theta_C + K_{II}(3\cos\theta_C - 1) = 0 \qquad (1)$$

where K_I and K_{II} are the modes I and II stress intensity factors respectively.

This crack curving criterion predicts a positive θ_C for a negative K_{II} since K_I is always positive as shown in Figure 4. Likewise, a negative θ_C is predicted for a positive K_{II}. In the absence of K_{II}, however, Equation (1) predicts a self similar crack propagation or $\theta_C = 0$ and fails to explain the physically observed crack instability where crack curving takes place in a K_I field. The static elastic crack curving criterion of Streit and Finnie (1980) or Ramulu and Kobayashi (1983) predicts such crack curving and was found to agree well with available experimental data. In the following, a brief account of a mode II extension of this crack curving theory is given.

The mixed mode, elastic crack tip stress field in terms of the crack tip polar coordinate system is given by

$$\sigma_{rr} = \frac{1}{\sqrt{2\pi r}}\cos\frac{\theta}{2}\left[K_I\left(1+\sin^2\frac{\theta}{2}\right)+\frac{3}{2}K_{II}\sin\theta - 2K_{II}\tan\frac{\theta}{2}\right]+\frac{\sigma_{ox}}{2}(1+\cos 2\theta)$$

$$\sigma_{\theta\theta} = \frac{1}{\sqrt{2\pi r}}\cos\frac{\theta}{2}\left[K_I\cos^2\frac{\theta}{2}-\frac{3}{2}K_{II}\sin\theta\right]+\frac{\sigma_{ox}}{2}(1-\cos 2\theta) \qquad (2)$$

$$\tau_{r\theta} = \frac{1}{2\sqrt{2\pi r}}\cos\frac{\theta}{2}\left[K_I\sin\theta + K_{II}(3\cos\theta - 1)\right]-\frac{\sigma_{ox}}{2}\sin 2\theta$$

where σ_{ox} is the second order term and is commonly referred to as the remote stress component. The same maximum circumferential stress criterion is then used to derive a mixed mode crack extension criterion by assuming that fracture will occur when the maximum circumferential stress is equal to the equivalent circumferential stress in mode I fracture. Experimental evidences compiled by Ramulu and Kobayashi (1983) heavily favors the incorporation of the second order term, i.e. Equation (3) in predicting the crack kinking angle under mixed mode fracture. The mixed mode fracture criterion of Equation (1) then becomes

$$K_{IC} = K_I\cos^3\frac{\theta_C}{2} - 3K_{II}\cos^2\frac{\theta_C}{2}\sin\frac{\theta_C}{2}+\frac{\sqrt{2\pi r}}{2}\sigma_{ox}(1-\cos 2\theta) \qquad (3)$$

Equation (3) incorporates the second order effect into Equation (1) but otherwise follows the general trend of Equation (1). If Equation (1) predicts a positive θ_C for a positive K_I and a negative K_{II}, Equation (3) shows that for the same K_I and K_{II} and positive σ_{ox}, $\theta_C = 0$ and the crack will propagate straight ahead. If $K_I > K_{II}$, Equation (3) also shows that for the same K_{II} and σ_{ox}, crack kinking is only possible when $K_I < K_{IC}$.

The crack kinking angle can be obtained by maximizing the circumferential stress and results in the following transcendental equation:

$$\frac{K_{II}}{K_I} = \frac{-\sin\frac{\theta_C}{2}}{(3\cos\theta_C - 1)}\left[2\cos\frac{\theta_C}{2} - \frac{16\sqrt{2\pi}}{3}\cdot A\cdot\cos\theta_C\right] \qquad (4)$$

$$A = \sqrt{r_C}\,\frac{\sigma_{ox}}{K_I} \qquad (5)$$

The term A, is related to the critical distance, r_C, from the crack tip and is proportional to the nonsingular stress, σ_{ox}. Ramulu and Kobayashi (1983) has shown that r_C is a material dependent parameter which must be determined experimentally. Thus, unlike the crack curving criterion represented by Equation (3), the crack kinking angle computed by Equation (4) incorporates the second order term and represents the mixed mode extension of crack kinking criterion of Streit and Finnie (1980) and Ramulu and Kobayashi (1983). As shown in Figure 5, the crack kinking angle, θ_C, increases with increasing σ_{ox} and negative σ_{ox} tends to stabilize the crack path.

The crack extension criterion represented by Equation (3) and the crack kinking criterion represented by Equation (4) does not account for the elevation in stress intensity factors, K_I and possibly K_{II}, due to the presence of MSD. The effect of MSD obviously is to promote self-similar crack extension, as seen in the NTSB report (1989), and can be incorporated into this analysis by artificially increasing K_I by a magnification factor which represents the interaction effect between the axial crack and the small crack emanating from the adjacent fastener hole.

Finally in the absence of an elastic-plastic crack curving criterion, the above elastic crack curving criterion was used to estimate the crack curving potential of a tear strap.

Results

Unlike the fuselage considered in [Kosai and Kobayashi (1991)], the crack flap is constrained from opening by the adjacent stringer which is 213 mm (8.4 in.) away from

the extending axial crack. The smaller flap opening in turn resulted in a small plastic yield zone at the crack tip as alluded to in previous sections.

As mentioned earlier, an elastic analysis was first conducted to study the extent of crack tip plastic yielding in order to determine the crack length at which incremental elastic-plastic analysis would be used with each increment of crack extension. This incremental analysis was initiated when the crack tip yield region reached the size of the crack tip element or at a crack length of 178 mm (7 in.). This elastic plastic analysis was conducted until the crack length reached a = 508 mm (20 in.). The resultant K_I, K_{II} for the limit pressure differential of 51.7 kPa (7.5 psi) computed by the coarse and fine grid finite element analyses are shown in Figures 6 and Figure 7, respectively. Also shown in these figures are K_I and K_{II} without the tear strap (TS), but with the stringer and frame. This FEM analysis models either a fuselage without a tear strap, or a fuselage with a disbonded tear strap.

Figure 6 shows that the first crack kinking occurred at 25.4 mm (1 inch) before the tear strap. The subsequent kinked crack analysis used a refined grid for each incremental crack extension while superposing successive numerical results on previous analyses. Figure 7 shows that the kinked crack propagated in a straight line after which it kinked again very close to the tear strap. While the predicted kinking angle without the non-singular stress, i.e. using Equation (1), is about θ_C = 30 degrees, the predicted kinking angle with the non-singular stress, i.e using Equation (4), is about θ_C = 40 degrees. Figure 6 also shows little differences in K_I and K_{II} with, and without, the tear straps.

Figure 9 shows the crack path obtained through this analysis. The results appear to agree qualitatively with those observed experimentally [Maclin (1991)]. Also shown in Figure 8 is the finite element idealization of the skin-stringer-frame construction.

Figure 8 shows the resultant K_I, K_{II} when a linearly varying cabin pressure, as shown in Figure 2, was prescribed on the crack flap. A comparison of Figures 6 and 9 shows negligible differences between the stress intensity factors associated with the different flap pressure. Thus details in the pressure distribution in the vicinity of the axial crack may be unimportant as long as the cabin pressure is maintained through the bulk of the fuselage during crack propagation.

The flap deformations due to the two pressure boundary conditions are shown in Figure 2. The fully pressurized flap deformed 9 mm (0.35 in.) more than the partially pressurized flap with little differences in the stress intensity factors as mentioned above.

Conclusions

The utility of large deformation, elastic-plastic finite element analysis with rezoning for predicting crack curving in a pressurized fuselage with tear straps was demonstrated. An

elastic crack propagation and kinking criteria in the presence of mixed mode fracture were presented.

Discussion

The large K_{II} and the large axial stress ahead of the propagating crack were developed through the large unsymmetric crack flap. For an airplane in flight, the high velocity air flow along the fuselage will tend to close the flap thus counteracting the effect of the opening flap due to cabin pressure. The net result is that the axial crack will continue to propagate without kinking and hence without arresting. Perhaps the large opening in the Aloha Airlines B737-200 [NSTB (1980)] could have been due in part to this air flow in flight which suppressed the development of crack flap necessary for crack curving and hence arrest.

Acknowledgement

The analysis reported in this paper was obtained under the sponsorship of ONR Contract N00014-89-J-1276. The authors wishes to express their gratitude to Dr. Y. Rajapakse for his continuing support through this investigation.

References

1. Kosai, M. and Kobayashi, A.S.: Axial Crack Propagation and Arrest in Pressurized Fuselage. Structural Integrity of Aging Airplanes. Eds. S.N. Atluri, S.G. Sampath and P. Tong, Springer-Verlag, (1991) 225-238.

2. Sampath, S. and Broek, D.: Estimation of Requirements of Inspection Intervals for Panels Susceptible to Multiple Site Damage. Structural Integrity of Aging Airplanes. Eds. S.N. Atluri, S.G. Sampath and P. Tong, Springer-Verlag, (1991) 339-389.

3. National Transportation Safety Board: Aircraft Accident Report. Aloha Airlines, Flight 243, Boeing 737-200, N73711, Near Maui, Hawaii, April 28, 1988, NTSB/AAR-89/03, 1989.

4. Fyfe, I.M. and Sethi, V.: The Role of Thin Cylinder Bulging on Crack Curvature. AIAA Paper 914086, 32nd Structures, Structural Dynamics and Materials Conference, Baltimore, MD, April 1991.

5. Kobayashi, A.S. and Engstrom, W.L.: Transient Analysis in Fracturing Aluminum Plate. Proceedings of JSME 1967 Semi-international Symposium, 172-182, 1967.

6. Arakawa, K., Drinnon, R.H., Jr., Kosai, M. and Kobayashi, A.S.: Dynamic Fracture Analysis by Dynamic Moire Interferometry. To be published in Experimental Mechanics.

7. Kobayashi, A.S., Emery, A.F., Love, W.J., Chao, Y.H. and Johannson, O.: Crack Bifurcation and Arrest in Pressurized Pipe. Fracture Mechanics: Nineteenth Symposium, ASTM STP 969, (1988) 441-465.

8. Kobayashi, A.S., Emery, A.F., Love, W.J. and Chao, Y.H.: Subsize Experiments and Numerical Modelling of Axial Rupture of Gas Transmission Lines. ASME Journal of Pressure Vessel Technology, 110, (1988), 155-160.

9. Erdogan, F and Sih, G.C.: On the Crack Extension in Plates Under Plane Loading and Transverse Shear. Journal of Basic Engineering 85 (1963) 519-527.

10. Streit, R. and Finnie, I.: An Experimental Investigation of Crack Path Directional Stability. Experimental Mechanics, 20,(1980) 17-23.

11. Ramulu, M and Kobayashi, A.S.: Dynamic Crack Curving - A Photoelastic Evaluation. Experimental Mechanics, 23, (March 1983) 1-9.

12. Ramulu, R and Kobayashi, A.S: Strain Energy Density Criterion in Elasticdynamic Mixed Mode Crack Propagation. Engineering Fracture Mechanics 18 (1983) 1087-1098.

13. Maclin, J.R.: A paper presented at the 1991 International Conference on Aging Aircraft and Structural Airworthiness, Washington, D.C.

ASK/cm/3/25/92

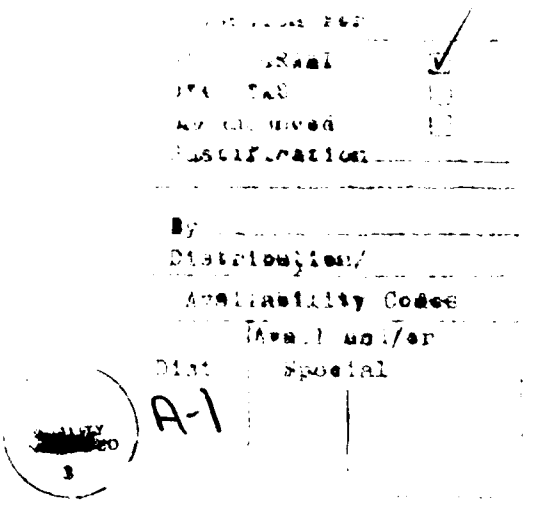

Parameter		Symbol	Value	
Skin & Tear Strap	Material	2024-T3 Clad Sheet		
	Thickness	t	0.9 mm	0.036 in
	Ultimate Strength	F_{tu}	427 MPa	62 ksi
	Yield Strength	F_{ty}	324 MPa	47 ksi
	Young's Modulas	E	72 GPa	10.5×10^{3} ksi
	Fracture Toughness	K_C	100 MPa $m^{0.5}$	91* ksi $in^{0.5}$
Fuselage Diameter		D	3759 mm	148 in
Tear Strap Spacing		S	254 mm	10 in
Tear Strap Width		W	50.8 mm	2 in
Frame Spacing		b	508 mm	20 in
Crack Length		2a	1016 mm	40 in
Limit Pressure Differential		P_{limit}	51.7 kPa	7.5 psi
Fail-Safe Pressure Differential		P_{fs}	62 .1kPa	9.0 psi

* Ref. MCIC-HB-01R, " Damage Tolerant Design Handbook "

Table 1. Structural and material property data for aircraft fuselage analysis

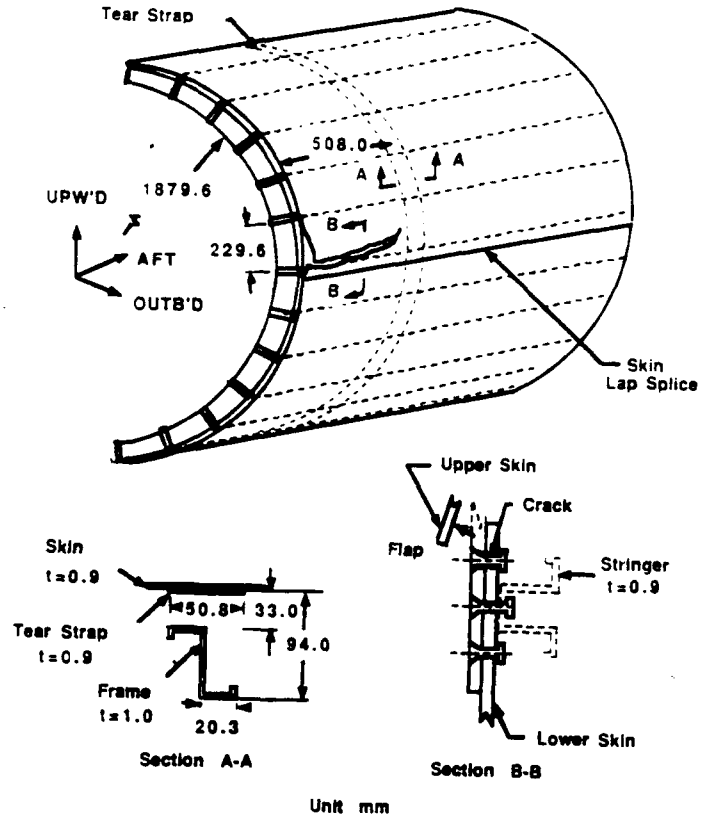

Figure 1. Axial rupture of an idealized fuselage.

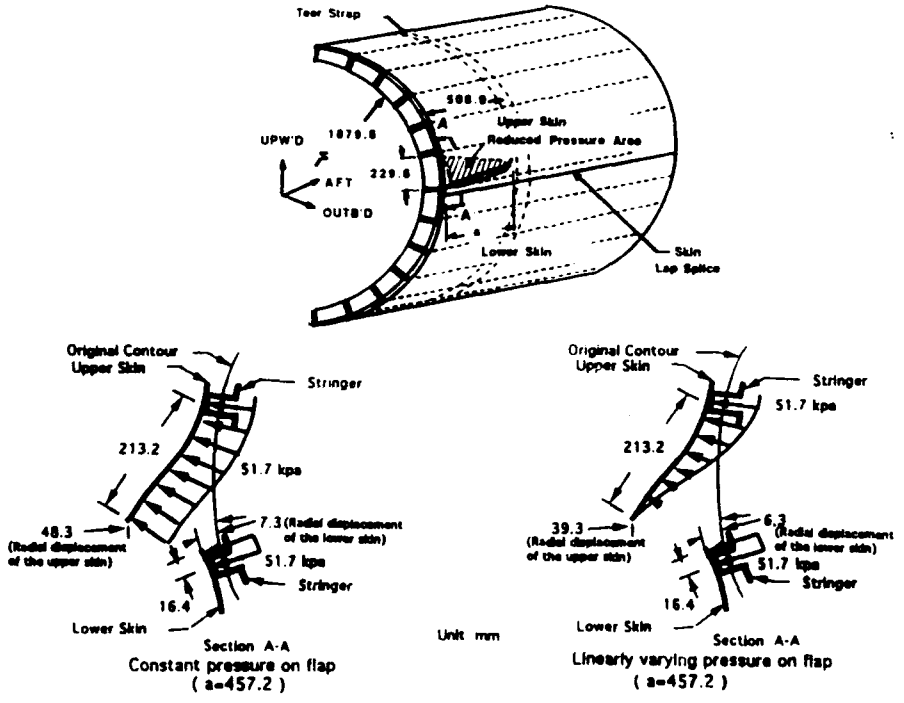

Figure 2. Estimated pressure on crack flap.

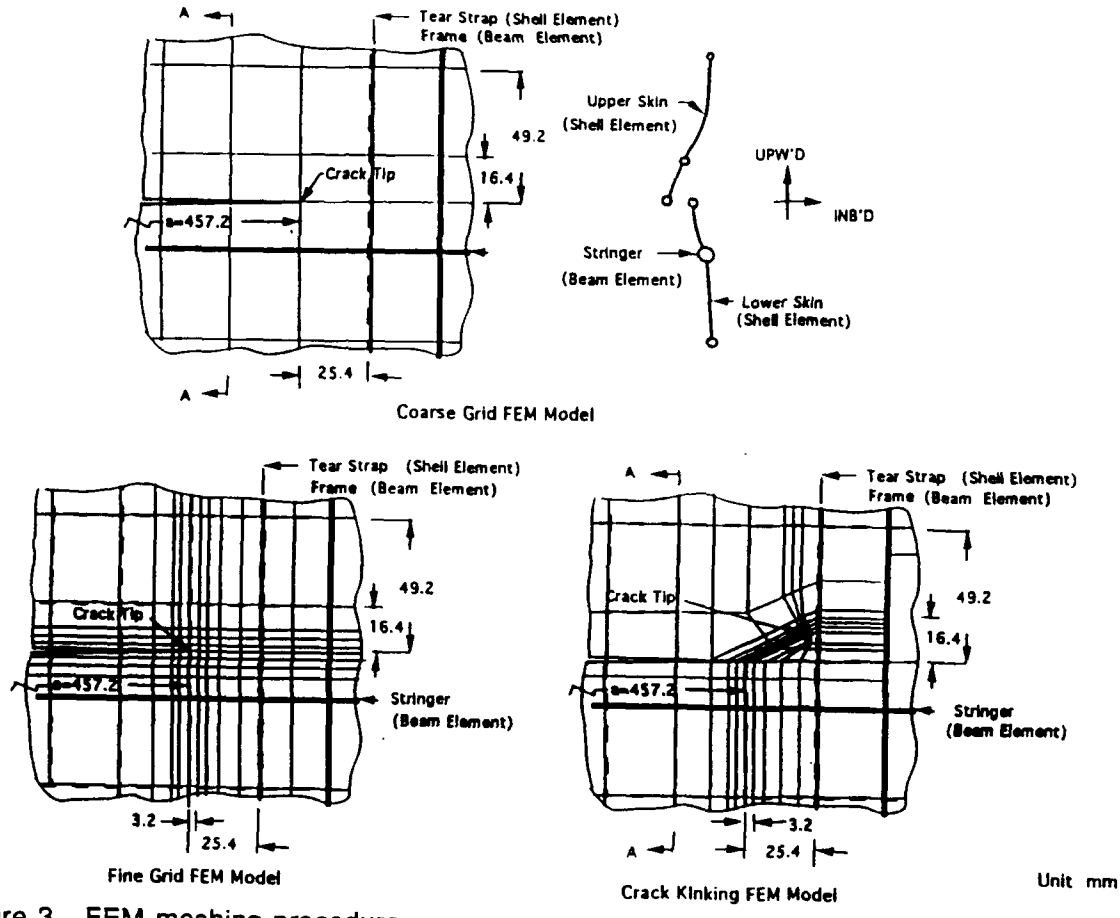

Figure 3. FEM meshing procedure

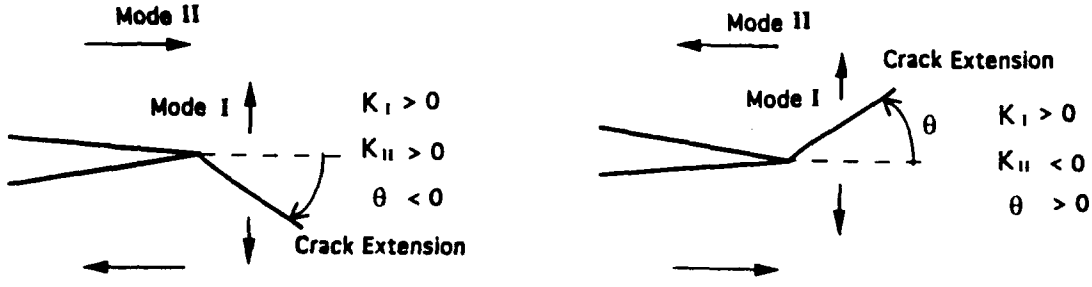

Figure 4. Crack extension angle under mixed mode loading.

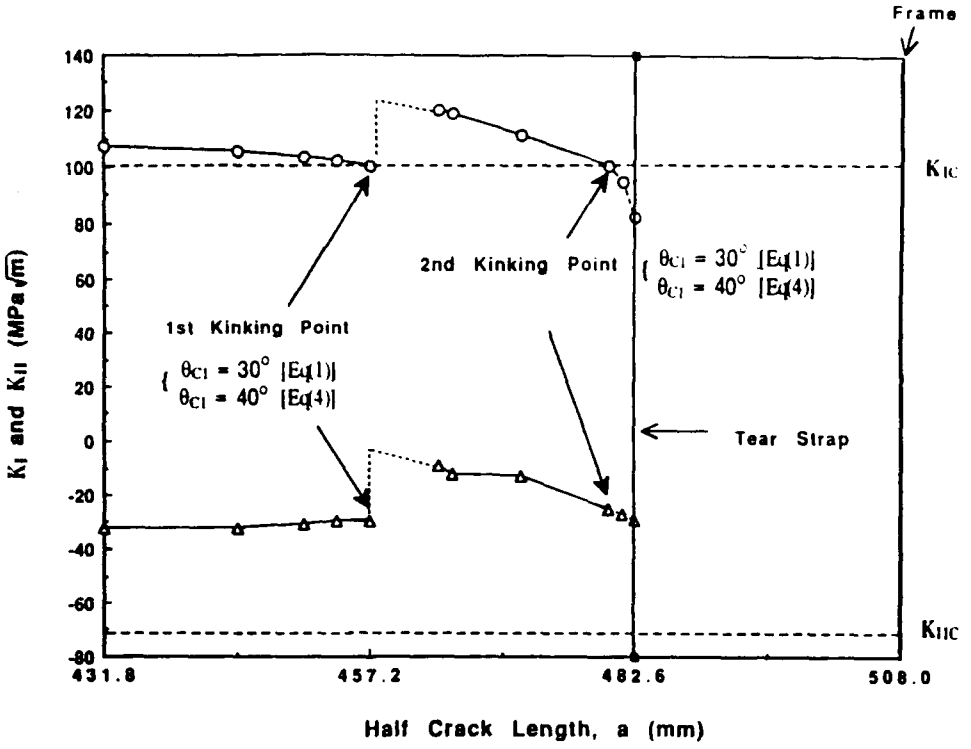

Figure 7. Stress intensity factor variations with crack extension (fine grid analysis). p = 51.7 kPa (7.5 psi).

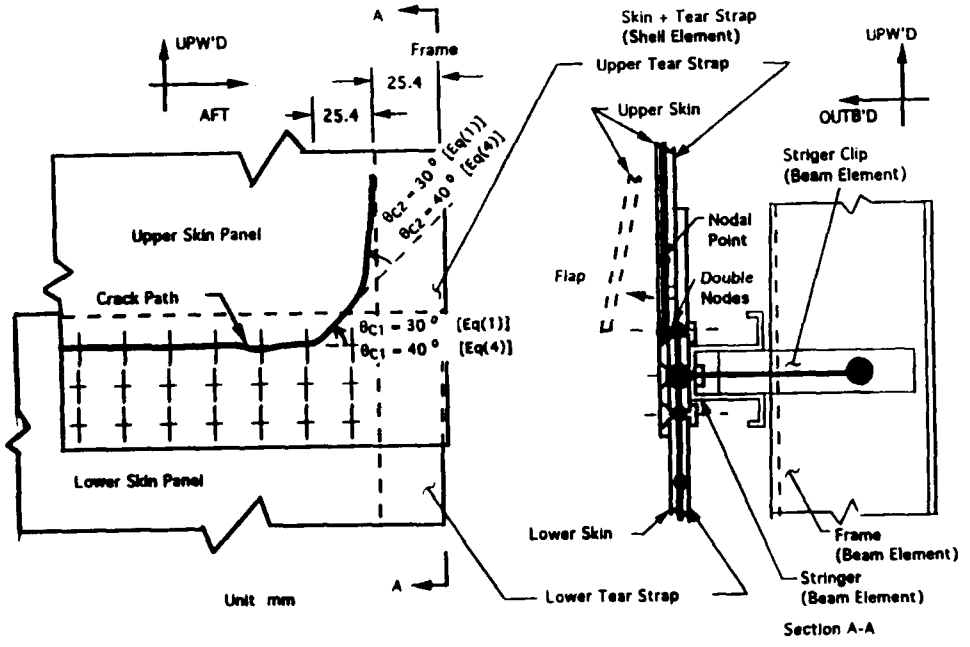

Figure 8. Crack path near tear strap and finite element idealization of skin-stringer-frame construction.

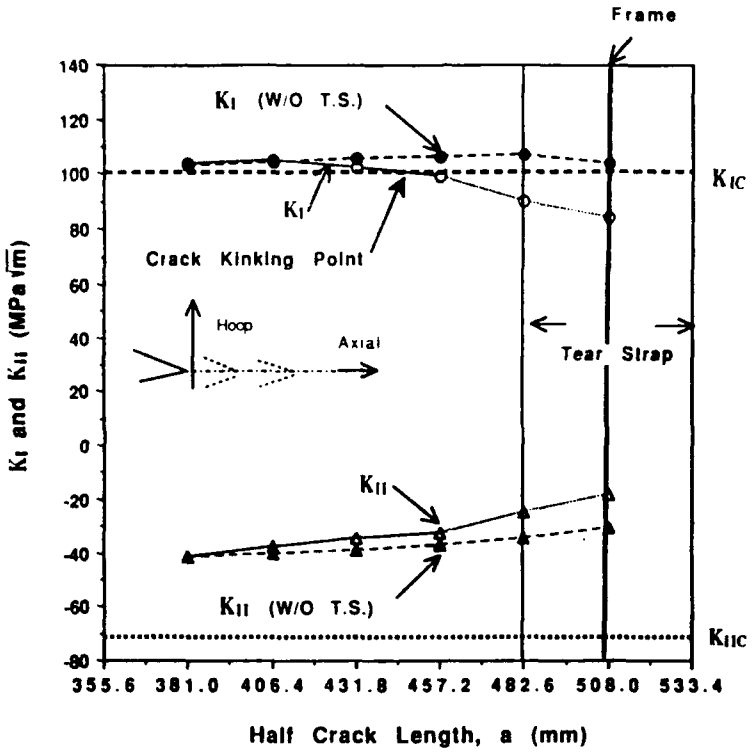

Figure 9. Stress intensity factor variation with crack extension. Linearly varying pressure on flap. p = 51.7 kPa (7.5 psi).

Unclassified

SECURITY CLASSIFICATION OF THIS PAGE (When Data Entered)

REPORT DOCUMENTATION PAGE		READ INSTRUCTIONS BEFORE COMPLETING FORM
1. REPORT NUMBER UWA/DME/TR-92/68	2. GOVT ACCESSION NO.	3. RECIPIENT'S CATALOG NUMBER
4. TITLE (and Subtitle) Tear Straps in Airplane Fuselage.		5. TYPE OF REPORT & PERIOD COVERED Technical Report 6. PERFORMING ORG. REPORT NUMBER UWA/DME/TR-92/68
7. AUTHOR(s) J. Kosai and A.S. Kobayashi		8. CONTRACT OR GRANT NUMBER(s) N00014-89-J-1276
9. PERFORMING ORGANIZATION NAME AND ADDRESS Department of Mechanical Engineering, FU-10 University of Washington Seattle, WA 98195		10. PROGRAM ELEMENT, PROJECT, TASK AREA & WORK UNIT NUMBERS
11. CONTROLLING OFFICE NAME AND ADDRESS Office of Naval Research Arlington, VA 22217		12. REPORT DATE March 1992 13. NUMBER OF PAGES 14
14. MONITORING AGENCY NAME & ADDRESS(if different from Controlling Office)		15. SECURITY CLASS. (of this report) 15a. DECLASSIFICATION/DOWNGRADING SCHEDULE

16. DISTRIBUTION STATEMENT (of this Report)

Unlimited

17. DISTRIBUTION STATEMENT (of the abstract entered in Block 20, if different from Report)

18. SUPPLEMENTARY NOTES

19. KEY WORDS (Continue on reverse side if necessary and identify by block number)

Elastic-plastic, fracture mechanics, crack arrest, tear straps, crack kinking.

20. ABSTRACT (Continue on reverse side if necessary and identify by block number)

A procedure based on dynamic fracture mechanics is proposed for assessing the effectiveness of tear straps in a rupturing airplane fuselage weakened by a row of multiple site damage (MSD). A large deformation, elastic-plastic finite element model of the rupturing fuselage with an unsymmetrical crack flap is used to demonstrate the existence of a mixed mode I and II crack tip deformation and a large axial stress preceding the propagating crack. These numerical results were used to evaluate the dynamic crack curving and crack arrest criteria and hence to assess the possibility of crack curving as the crack approaches a tear strap without the presence of MSD.

DD FORM 1 JAN 73 1473 EDITION OF 1 NOV 65 IS OBSOLETE
S/N 0102-014-6601

unclassified

SECURITY CLASSIFICATION OF THIS PAGE (When Data Entered)